Two-dimensional optical tomography of hemodynamic changes in a preterm infant brain

Feng Gao (高 峰)[1], Yuan Xue (薛 媛)[1], Huijuan Zhao (赵会娟)[1], Takashi Kusaka[2], Masanori Ueno[3], and Yukio Yamada[3]

[1] *College of Precision Instrument and Optoelectronics Engineering, Tianjin University, Tianjin 300072*

[2] *Faculty of Medicine, Kagawa University, Kagawa 761-0793, Japan*

[3] *Department of Mechanical Engineering and Intelligent Systems, University of Electro-Communications, Tokyo 182-8585, Japan*

Received November 7, 2006

Our preliminary results on two-dimensional (2D) optical tomographic imaging of hemodynamic changes in a preterm infant brain are reported. We use the established 16-channel time-correlated single photon counting system for the detection and generalized pulse spectrum technique based algorithm for the image reconstruction. The experiments demonstrate that diffuse optical tomography may be a potent means for investigating brain functions and neural development of infant brains in the perinatal period.

OCIS codes: 170.3880, 170.5280, 170.3010, 170.1470.

Diffuse optical tomography (DOT) is a non-invasive imaging modality that can significantly improve the quantitative performances of near-infrared (NIR) spectroscopy and extend its ability to localize hemodynamic variations within tissue[1]. Because of the relatively low absorption, thin skull, small dimension and relatively low probability of movement, preterm infant brains are the most suitable targets to be safely and continuously imaged with DOT. On the other hand, current unavailability of a feasible means for non-invasively and quantitatively assessing regional cerebral perfusion and oxygenation in infant brains has been motivating the desire to apply optical technique for the purpose. For the past ten years, the efforts to develop a NIR spectroscopic imaging modality of neonate brains have been primarily pioneered by the researchers of University College London, where several experiments of three-dimensional (3D) DOT have been conducted to demonstrate the potentials of this technique in diagnosis of cerebral hypoxic-ischemic injury and imaging of brain function in preterm infants[2−4]. Nevertheless, due to the lack of "gold standard", researchers in other groups are strongly encouraged to repeat the experimental procedures with similar and/or different protocols to validate the effectiveness of the technique and to identify the direction for the further improvement in the methodology. In this paper, we report our first results on tomographic imaging of hemodynamic changes in a preterm infant brain induced by alterations to ventilator settings. The experiments employed an established 16-channel time-correlated single photon counting (TCSPC) system for the time-resolved measurement[5] and a specific two-dimensional (2D) algorithm based on the generalized pulse spectrum technique (GPST) for the image reconstruction[6].

The system used in the experiment is a lab-assembled 16-channel time-resolved NIR optical imaging system, which is essentially based on a TCSPC technique. Two $\sim$ 100-ps pulsed laser diodes (LDs) with a repetition rate of 5 MHz and an average power of about 0.25 mW emit NIR lights at wavelengths of 760 and 830 nm, respectively. The lights are then differently delayed with an interval of about 25 ns and jointly sent to the 16 source fibers through a 1:16 optical switch. In such a way, the times-of-flight of the re-emitted photons at the two wavelengths can be measured simultaneously. The optodes adopt a coaxial structure for source and detection fibers, where a single fiber of 400 μm in diameter at the inner core is used for illumination and a bundle of small fibers of 30 μm at the annulus for detection. Each channel contains a custom-made optical attenuator between the detection fiber bundle and the photomultiplier tube (PMT). The attenuation degrees of all the attenuators need to be adjusted successively channel by channel to give appropriate light intensities for all the PMTs to work at a reasonable photon-counting rate, prior to the measurement. The photons re-emitted from the object surface are collected simultaneously by all the detection fiber bundles and then temporarily resolved by the 16 parallel TCSPC units with electronic resolution of about 15 ps, for each of the 16 alternatively illuminating source-pairs of the two wavelengths and for a given integration time. As a result, a set of 256 histograms of the photon flight times that are proportional to the realistic temporal point spread functions (TPSFs) is accumulated and, furthermore, analyzed for the image reconstruction.

The image reconstruction process in the experiment is based on the GPST nonlinear scheme, by which we mean Laplace-transforming the time-dependent signals into a real frequency domain and inverting the real frequency domain components. Physically, the Laplace transform using a positive or negative real frequency can be interpreted as exponential time weighting that favors "early-time" and "late-time" features of the time-resolved re-emissions. With such a way, it is possible to achieve an optimum signal-to-noise ratio (SNR) through selectively amplifying the rear parts of the curves that mostly characterize the inner heterogeneous variations while maintaining an acceptable noise level. The main framework of the diffusion-GPST algorithm is the linearization of the original nonlinear inverse problem by a Newton-Raphson

1671-7694/2007/080472-03

scheme, forming an outer loop of an iterative procedure,

$$\mathbf{\Gamma}_m - \mathbf{F}(\boldsymbol{\mu}_k) = \mathbf{J}(\boldsymbol{\mu}_k)\,\delta\boldsymbol{\mu}_k, \quad \boldsymbol{\mu}_{k+1} = \boldsymbol{\mu}_k + \delta\boldsymbol{\mu}_k, \qquad (1)$$

where $\mathbf{\Gamma}_m$ is a column vector numerating the Laplace-transformed re-missions for all the source-detector pairs and transforming frequencies, i.e. the measured datatype; $\mathbf{F}$ is the forward operator associated with the solution to the Lapalace-transformed photon diffusion equation by using a Galerkin finite element method (FEM); $\boldsymbol{\mu}_k$ and $\delta\boldsymbol{\mu}_k$ are the vectors denoting the absorption coefficient at the nodes of the FEM mesh and its update, at the kth iteration; $\mathbf{J}$ is the Jacobian matrix of $\mathbf{F}$, which can be efficiently calculated using a perturbation technique and needs to be updated at each stage[6]. Finally the resultant linear equation is weight-scaled and solved using an algebraic reconstruction technique.

Informed parental consent was obtained to perform the investigation on a 32-day-old female preterm infant with gestational age of 32 weeks and a weight of 1065 g. As part of the intensive care of an extremely low birth weight infant of 998 g, she required mechanical ventilation. Figure 1 illustrates the 2D arrangement of the optodes in the experiment, where two semi-circular plastic fiber-holders of 90 mm in diameter, each holding 8 optodes with equal spacing, are connected through 15-nm-thick rubber mats to adapt to the head shape. An essential requirement for the model-based image reconstruction is prior knowledge of the spatial coordinates of all the sources and detectors on the head. In our practice, the coordinates of the optodes is calculated by simple geometrical arithmetic, according to the lengths of the optode segments penetrating into the holder that are measured immediately after the experiment. A spline interpolation procedure is applied to the optode coordinates to obtain the refined description of the head boundary, from which a discretizing mesh of the imaging plane, consisting of 2780 triangular elements and 1519 nodes, is constructed for the later FEM forward and inverse calculations, as shown in Fig. 2.

Following a period of 12 min after attaching the fiber-holder to the infant, a set of data was acquired using an acquisition time of 5 s per illuminating source. The ventilation settings during this first baseline (rest-state) measurement corresponded to a partial pressure of oxygen of $P_{O_2} \approx 96$ mmHg and a partial pressure of carbon diode of $P_{CO_2} = 32 - 36$ mmHg. Thereafter a task-state measurement was done for the same acquisition time and attenuation setting as those of the rest-state, as P_{O_2} was increased to around 100 mmHg and P_{CO_2} decreased

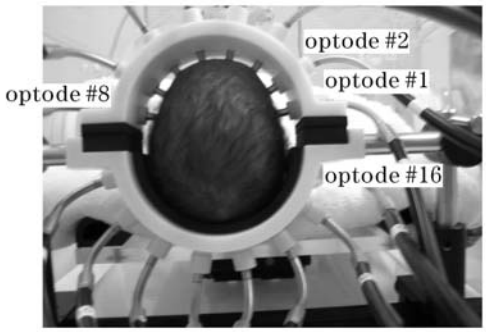

Fig. 1. Arrangement of optodes in the experiment.

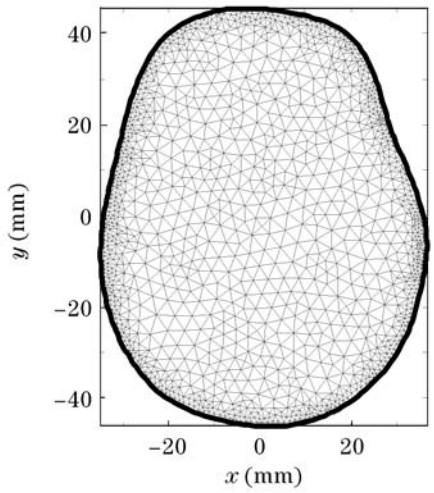

Fig. 2. FEM mesh from the spline-interpolated boundary.

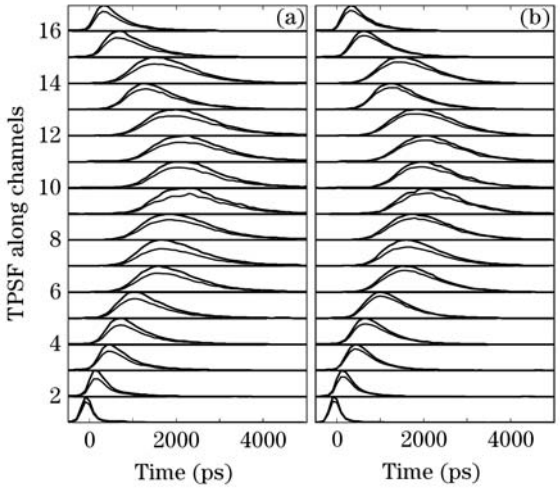

Fig. 3. TPSFs at the two wavelengths measured by the 16 detectors for the first source, (a) at 760 nm and (b) at 830 nm. The thick lines are for the task state and light lines for the rest state.

below 29 mmHg by increasing the respiration rate from 170 to 180 min^{-1}. Figure 3 shows the TPSFs measured by the 16 detection channels for the first source in the experiment, and Fig. 4 depicts the ventilation settings during the series of tomographic scans. The whole TPSF set was analyzed to exclude the data with low SNR, particularly those measured across the largest diameter of about 90 mm, from the reconstruction process.

In this study we aim at imaging the hemodynamic changes in the infant brain in response to the alterations of the ventilation settings. For this purpose a so-called difference imaging scheme can be employed, which reconstructs the images at the two wavelengths from the differences or ratios in the data-types resulting from the measurements before and after the alterations to the ventilation settings. With regard to the GPST algorithm aforementioned, the measured data-type to be fitted is constructed as

$$\Gamma_m = (\Gamma_{\text{task}}/\Gamma_{\text{rest}})\Gamma(\boldsymbol{\mu}_0), \qquad (2)$$

where Γ_{rest} and Γ_{task} are the Laplace-transformed re-emissions measured at the rest and task states,

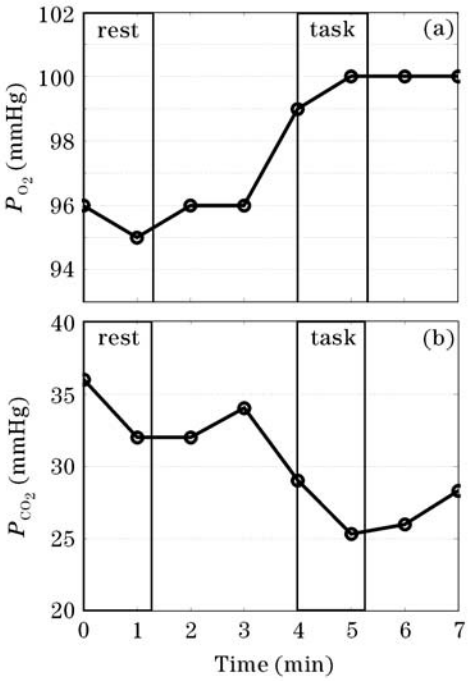

Fig. 4. Experimental conditions during tomographical scan. (a) P_{O_2}; (b) P_{CO_2}.

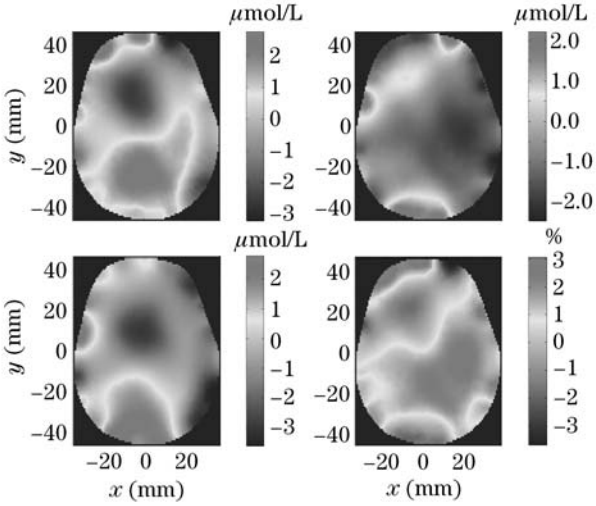

Fig. 5. Reconstructed images of hemodynamic changes. (a) [ΔHbO$_2$]; (b) [ΔHbR]; (c) [ΔHbT]; and (d) ΔS_{O_2}.

respectively; $\Gamma(\boldsymbol{\mu}_0)$ is the model prediction according to the initial settings of the normal hemodynamic state in neonatal brains: a total hemoglobin concentration of [HbT] = 65 μmol/L, an oxygen saturation of S_{O_2} = 70%, and a reduced scattering coefficient of μ_s' = 0.65 mm^{-1}[7]. With such a difference imaging scheme, not only the requirements for accurate positions of the optodes and baseline optical parameters become significantly less severe, but also the absolute measurement of the Laplace-transformed re-emissions can be used that is proved highly robust to the image reconstruction. Most importantly, it enables application of a 2D algorithm to the realistic 3D situation since the ratio of the task-state data-type to the rest-state one has been shown to be approximately equal for 2D and 3D cases by simulations[8].

The reconstructed images of the hemodynamic changes in the neonatal brain at the imaging plane are exhibited in Fig. 5. As expected, decreasing P_{CO_2} caused lower global absorption due to the decreased cerebral blood volume — this effect can be seen as an evident decrease in [HbT] in the central region of the brain. As a result of the increased P_{O_2}, a decrease in the deoxy-hemoglobin concentration ([HbR]) and correspondingly an increase in S_{O_2} in right-rear region of the brain can be clearly observed. Also, we observed a considerable increase in the rear region of the imaging plane and an evident decrease in the central region, in oxy-hemoglobin concentration ([HbO$_2$]). The reasonable justification and explanation for the observations need a further investigation through a series of repetitive experiments. It is very important to note that the significant changes (either positive or negative) in the boundary regions of all the images should be ascribed to the artifacts during the reconstruction process since it is less likely for hemodynamic changes to occur in the skull and cerebrospinal fluid layers.

In summary, we have obtained our preliminary images of hemodynamic changes in a preterm infant brain in response to ventilation settings using our established 16-channel TCSPC measuring system and specific image reconstruction algorithm based on the GPST diffusion model. The results reasonably agree to the physiologically expected global changes in blood volume and oxygenation, demonstrating time-resolved DOT as a promising way of monitoring neural development in the neonatal brain. A series of repetitive experiments are required for the full validation of the methodology.

F. Gao, Y. Xue, and H. Zhao acknowledge the supports from the National Natural Science Foundation of China (No. 60478008, 60678049) and the National Basic Research Program of China (No. 2006CB705700). T. Kusaka, M. Ueno, Y. Yamada, and F. Gao acknowledge the fund from the Ministry of Education, Culture, Sports, Science and Technology of Japan (No. 13777212). F. Gao also thanks the Japan Society for the Promotion of Science for providing a short-term fellowship (No. S06093). F. Gao's e-mail address is gaofeng@tju.edu.cn.

References

1. S. R. Arridge, Inverse Problems **15,** R41 (1999).
2. J. C. Hebden, A. Gibson, R. M. Yusof, N. Everdell, D. T. Delpy, S. R. Arridge, T. Austin, J. H. Meek, and J. S. Wyatt, Physics in Medicine and Biolology **47,** 4155 (2002).
3. J. C. Hebden, A. Gibson, T. Austin, R. M. Yusof, N. Everdell, D. T. Delpy, S. R. Arridge, J. H. Meek, and J. S. Wyatt, Physics in Medicine and Biology **49,** 1117 (2004).
4. A. P. Gibson, T. Austin, N. L. Everdell, M. Schweiger, S. R. Arridge, J. H. Meek, J. S. Wyatt, D. T. Delpy, and J. C. Hebden, NeuroImage **30,** 521 (2006).
5. H. Eda, I. Oda, Y. Ito, Y. Wada, Y. Oikawa, Y. Tsunazawa, M. Takada, Y. Tsuchiya, Y. Yamashita, M. Oda, A. Sassaroli, Y. Yamada, and M. Tamura, Rev. Sci. Instrum. **70,** 3595 (1999).
6. F. Gao, Y. Tanikawa, H. Zhao, and Y. Yamada, Appl. Opt. **41,** 7346 (2002).
7. S. Ijichi, T. Kusaka, K. Isobe, K. Okubo, K. Kawada, M. Namba, H. Okada, T. Nishida, T. Imai, and S. Itoh, Pediat. Res. **58,** 568 (2005).
8. H. Zhao, F. Gao, Y. Tanikawa, K. Homma, and Y. Yamada, Appl. Opt. **44,** 1905 (2005).